EPSC Abstracts
Vol. 13, EPSC-DPS2019-1359-2, 2019
EPSC-DPS Joint Meeting 2019

EPSC
EPSC-DPS Joint Meeting 2019
15–20 September 2019 | Geneva, Switzerland

A new map of thermal variations with depth within Copernicus crater using Chang'E-2 (CE-2) Microwave RadioMeters (MRMS) data

Roberto Bugiolacchi (1,2), Guoping Hu (1) and Kwing Lam Chan (1)
(1) MUST, SKLplanets, Macau, China (rbugiolacchi@must.edu.mo), (2) University College London, London, UK

Abstract

Microwave data from the Chinese lunar missions CE-1 and CE-2 offer new insights into the surface and near-sub-surface composition and physical properties. Calibration issues have slowed the release of science products; however, these are being presently addressed (see [12]) and this analysis gives an inkling of the great potential for new geophysical understandings.

Introduction

By its longer wavelength in comparison to UV-VIS-IR, microwave radiation carries information from deeper into the surface and can extend to several times the observation wavelength. Moreover, passive microwave measurements can be carried out during night time and in shadowed regions. Most observations of the lunar surface in these frequencies were Earth-based but they helped develop theoretical models to obtain the brightness temperature (TB) of the lunar surface and derive several of physical parameters including heat flow [5]. Here, we preview the results from a new investigative approach that takes advantage of global lunar microwave data obtained from the Chang'E-2 mission (CE-2) focusing on crater Copernicus.

Data and Method

The Level 2C Chang'E-2 (CE-2) Microwave RadioMeter (MRMs) data [13-7] was used in this study, following system calibration and geometric correction with Planetary Data System [6]. The MRM underwent onboard adjustments to ensure its reliability and accuracy using a two-point calibration method (for details see [13-2-11]). We used spherical harmonic fits for the Brightness Temperature (TB) variations with local time [11] to suppress the lunar phase effect. Normalized TBs at midnight were chosen to minimise the topographic effects on the emission [4].

We selected the widest range possible of data from the four frequencies available (3 GHz, T1, and 37 GHz, T4) to compare the average thermal emission at different depths within the lunar regolith at midnight (centimetres range for T4, 0.81 cm wavelength, to several meters T1, 10 cm wavelength). The penetration depth mainly depends on wavelength but also on the bulk density and loss tangent of the lunar regolith. We subtracted T4 from T1 to focus on the subsurface temperature variations with a surface resolution of around 6 km/px (TB_{diff}, Fig. 1A). One of the advantages of using a subtractive technique is the sharpening of boundary definition by a bucking effect: the subtraction minimizes the absolute value error caused by the calibration issues in some degree since the errors are found to be systematic at each channel [7].

Results

Copernicus crater has been the subject of many dedicated studies, even a proposed Apollo landing site. The diverse morphology of its rim (slumped southern terraces and ejecta apron, see Fig. 1-B in [4]). has been mostly attributed to a low-angle impact from the south-east.

The interior of large Copernican craters appears as microwave "hot spots" during daytime and "cold spots" during night time [14]. [3] proposed that the abundance of rocks in the interior would influence the diurnal change of MW and IR thermal emissions; these could be correlated with the age of the impact and used as a diagnostic tool.

The TB_{diff} map reveals that unlike other large young crates in the region (e.g., Aristarchus), Copernicus' MW emissions are anisothermal along its rim and interior (Fig. 1-A). The distribution is highly asymmetrical with very low values across the location of the "A wedge" [9] and high values (~40 K) around the southern rim.

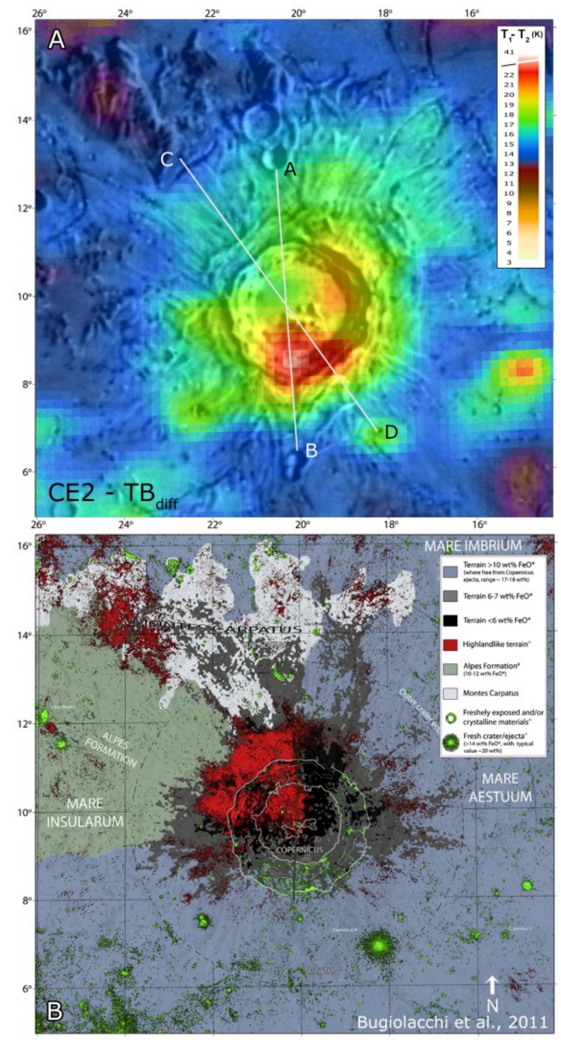

Figure 1. A] TBdiff in the Copernicus crater region superimposed on a shaded relief map [10]; B] Geological map highlighting FeO (wt%) variations and fresh materials [1].

The highest brightness temperatures differences within the crater floor match the surface roughness morphology, described as 'hummocky' (Ccfh) in geological maps [8] and in contrast with the 'smooth' wedge (Ccfs). Thus, as a preliminary conclusion, it appears that the surface's physical properties such as roughness and rockiness to be the leading factors influencing the microwave signature from the subsurface.

Discussion

[9] propose that the north-western segment ("red spot") be due to the higher silicic content of the ejecta. [1] had also noted FeO (wt%) variances in the Copernicus quadrant with values ranging from very low values (<6%, 'red and black') in the northern half of the edifice and nearby ejecta to 'mare background' levels in the south (>10%), Fig. 1-B.

Further, the spectral data reveal a local presence in the southern rim of materials exhibiting a strong 1 μm absorption feature, usually diagnostic of less weathered or even fresh mafic materials. This could originate from an enhanced fragmentation of the wall materials due to mechanical properties of the local rocks and steeper slopes and/or their relative higher mafic content. The TB_{diff} data, therefore, support the hypothesis that the impactor might have hit a heterogeneous target region, exhuming different ejecta materials. Thus, the reason for the anisothermal TB_{diff} values around the crater rim might be due to both morphological differences brought about by an enhanced gravitationally-led slumping rate in the southern part of the rim, creating a larger population of fractured rocks, and compositional, due to its relatively higher mafic content against the silicic north-western 'wedge'.

References

[1] Bugiolacchi et al., (2011) Icarus, 213, 43-63.
[2] Chan K. L. et al. (2010) Earth and Planet. Sci. Lett., 295, 1-2, 287-291.
[3] Gong, X, Y-Q Jin (2013) Acta Astr., 86, 237-246
[4] Hu G. et al. (2017) Icarus, 294, 72-80.
[5] Keihm S. J. and Langseth M. G. (1975) Science, 187, 64-66.
[6] McMahon S. K. (1996) P& SS, 44, 3-12.
[7] NAO, CAS, accessed Feb 29, 2016. //moon.bao.ac.cn/ceweb/datasrv/dmsce1.jsp.
[8] Schmitt H.H. et al. (1967) US Geol. Surv. Misc. I-515 (LAC-58).
[9] Shkuratov Y. et al. (2016) Icarus, 272, 125-139.
[10] U.S. Geol. Survey, I-2769.
[11] Wang Z. Z. et al. (2010) Science China: Earth sciences. 53, 1392-1406.
[12] Wei G, et al., (2019) Journal of Geophysical Research: Planets, 124.
[13] Zheng Y. C. et al. (2012) Icarus, 219, 194-210.
[14] Zheng Y-C et al., (2018) Icarus, 319, 627-644.